Elsevier Editorial System(tm) for
NeuroImage: Clinical

Manuscript Draft

Manuscript Number:

Title: Differential intrinsic functional connectivity changes in three language networks in Semantic Primary Progressive Aphasia

Article Type: Regular Article

Section/Category: Dementia

Corresponding Author: Dr. Giovanni battistella,

Corresponding Author's Institution: UCSF

First Author: Giovanni battistella

Order of Authors: Giovanni battistella; Maya Henry; Benno Gesierich; Stephen M Wilson; Valentina Borghesani; Wendy Shwe; Zachary Miller; Jessica Deleon; Bruce L Miller; Jorge Jovicich; Nico Papinutto; William W Seeley; Maria Luisa Mandelli; Maria Luisa Gorno-Tempini

Abstract: The semantic variant of primary progressive aphasia (svPPA) is a clinical syndrome characterized by selective neurodegeneration of anterior temporal regions underlying semantic memory with relatively preserved motor speech, syntax and phonology. Speech production, semantics, and orthography are fundamental domains of language processing. However, characterization of intrinsic connectivity in brain networks associated with each of these cognitive mechanisms and their dynamic changes in neurodegenerative disorders is lacking. The left inferior parietal lobule (IPL) is a crucial hub of the language network, characterized by widespread neural connectivity to other left-hemisphere nodes. The IPL is not severely damaged in svPPA, and we hypothesized that an enhanced connectivity pattern in this region might be related to the unusual dissociation of language functions typically seen with this disorder.
Using whole-brain, seed-based connectivity on Magnetic Resonance Imaging (MRI) resting-state data, we first identified three networks with differential IPL connectivity in 32 healthy controls. These networks consisted of a dorsal phonological-articulatory system involving inferior frontal and supramarginal regions; a ventral semantic network involving anterior middle temporal and angular gyri; and a third involved in direct orthography-to-phonology conversion linking posterior inferior temporal and intraparietal regions. We then compared activity of these three networks between 16 svPPA patients and the 32 age-matched controls. In svPPA patients, decreased functional connectivity in the ventral semantic network correlated with weak semantic skills, while orthographic network connectivity correlated with pseudoword reading skills. Increased connectivity between the inferior frontal gyrus and the superior portion of the angular gyrus suggested possible adaptive changes.
Our findings support a functional subdivision of the left IPL based on its connectivity to specific language-related regions. Moreover, the unique neuroanatomical and linguistic profile observed in svPPA provides a compelling model for the functional interplay of these networks, being either up or down regulated in response to disease.

Suggested Reviewers: Argye Hillis
Johns Hopkins Medicine
ahillis@jhmi.edu

Stanislas Dehaene
Unité Inserm-CEA de NeuroImagerie
Stanislas.Dehaene@cea.fr

Matthew Lambon Ralph
The University of Manchester
matt.lambon-ralph@manchester.ac.uk

Steven L Small
University of California, Irvine
small@uci.edu

Gregory S Hickock
University of California, Irvine
gshickok@uci.edu

Opposed Reviewers:

1. Cover Letter

University of California
San Francisco

Department of Neurology
Memory and Aging Center

Giovanni Battistella, Ph.D
Postdoctoral Fellow
UCSF Memory and Aging Center
Department of Neurology
Mission Hall Building
550 16th street, Room 5131
San Francisco, CA, 94158
Tel: 415-502-3804
Email: giovanni.battistella@ucsf.edu

19th October 2018

Dear Editor,

We are pleased to submit our manuscript entitled "Differential intrinsic functional connectivity changes in three language networks in Semantic Primary Progressive Aphasia" to be considered for publication as an original article in *Neuroimage:Clinical*.

Language processing is supported by multiple brain networks that control specific language functions, including speech production, semantics, and orthography. However, characterization of intrinsic connectivity in brain networks associated with each of these cognitive mechanisms, as well as their changes in neurodegenerative disorders, is lacking. Using MRI resting-state data, we studied functional connectivity in three brain networks anchored to seed regions fundamental to these language functions. We assessed the connectivity of these networks in healthy controls and patients with the semantic variant of primary progressive aphasia (svPPA), a focal neurodegenerative disease associated with profound semantic deficits and spared articulation/phonological processing. Our findings indicate that the left inferior parietal lobule (IPL) is a major hub in which all three networks converge, with a tripartite division of the language system into distinct sub-regions. Furthermore, our data provide evidence that changes in functional connectivity of the IPL reflect not only the behavioral impairments observed in svPPA, but also possible neural adaptations. The unique neuroanatomical and linguistic profile observed in svPPA provides a compelling model for the functional interplay of these networks, reflecting up-or down-regulation in response to disease.

We hope that, in light of these findings, our manuscript will be of interest to the Editorial board and the readers of *Neuroimage:Clinical*. The author certifies that all co-authors have participated sufficiently in the work to take responsibility for the whole content of the manuscript. Moreover, we attest that this work is not under review at any other publication and take responsibility for the integrity of the data and the accuracy of the data analyses.

Thanks for your valuable time, and we look forward to hearing from you.

Yours sincerely,

Giovanni Battistella (on behalf of all the co-authors of the manuscript)

Reviewer suggestions

1- Argye Hillis, M.D.
Johns Hopkins Medicine
ahillis@jhmi.edu

2- Stanislas, Dehaene, Ph.D.
Unité Inserm-CEA de NeuroImagerie
Stanislas.Dehaene@cea.fr

3- Matthew Lambon-Ralph, Ph.D.
The University of Manchester
matt.lambon-ralph@manchester.ac.uk

4- Steve L. Small, M.D., Ph.D.
University of California, Irvine
small@uci.edu

5- Gregory Hickock, Ph.D.
University of California, Irvine
gshickok@uci.edu

Highlights

- We identified 3 segregated left hemisphere language networks in healthy controls
- These networks were connected to discrete areas within the inferior parietal lobule
- SvPPA patients showed up- and down- regulation of the dorsal and ventral pathways
- SvPPA provides a compelling model for the functional interplay of these networks

Differential intrinsic functional connectivity changes in three language networks in Semantic Primary Progressive Aphasia

Giovanni Battistella[1], Maya Henry[1,2], Benno Gesierich[1], Stephen M. Wilson[3], Valentina Borghesani[1], Wendy Shwe[1], Zachary Miller[1], Jessica Deleon[1], Bruce L. Miller[1], Jorge Jovicich[4], Nico Papinutto[5], William W. Seeley[1], Maria Luisa Mandelli[1], Maria Luisa Gorno-Tempini[1]

[1]Memory and Aging Center, Department of Neurology, University of California, San Francisco, CA 94158, USA

[2]Speech, Language and Hearing Sciences, University of Arizona, Tucson, AZ 85721, USA

[3] Department of Hearing and Speech Sciences, Vanderbilt University Medical Center, Nashville, TN 37232, USA

[4]Center for Mind/Brain Sciences (CIMeC), University of Trento, Rovereto, Italy.

[5]Department of Neurology, University of California, San Francisco, CA 94158, USA

CORRESPONDING AUTHOR

Giovanni Battistella, UCSF Memory and Aging Center, Mission Hall Building, 505 16th street, Room 5131, San Francisco, CA 94158, USA. E-mail: Giovanni.battistella@ucsf.edu

RUNNING TITLE: Intrinsic language networks in svPPA.

KEYWORDS: Primary progressive aphasia, functional connectivity, resting-state connectivity, language, parietal lobe**.**

Numbers: 30 pages; 5 figures; 2 tables.

Word Count: Manuscript 4547**;** Abstract 297; Introduction 617; Discussion 1599.

ABSTRACT

The semantic variant of primary progressive aphasia (svPPA) is a clinical syndrome characterized by selective neurodegeneration of anterior temporal regions underlying semantic memory with relatively preserved motor speech, syntax and phonology. Speech production, semantics, and orthography are fundamental domains of language processing. However, characterization of intrinsic connectivity in brain networks associated with each of these cognitive mechanisms and their dynamic changes in neurodegenerative disorders is lacking. The left inferior parietal lobule (IPL) is a crucial hub of the language network, characterized by widespread neural connectivity to other left-hemisphere nodes. The IPL is not severely damaged in svPPA, and we hypothesized that an enhanced connectivity pattern in this region might be related to the unusual dissociation of language functions typically seen with this disorder.

Using whole-brain, seed-based connectivity on Magnetic Resonance Imaging (MRI) resting-state data, we first identified three networks with differential IPL connectivity in 32 healthy controls. These networks consisted of a dorsal phonological-articulatory system involving inferior frontal and supramarginal regions; a ventral semantic network involving anterior middle temporal and angular gyri; and a third involved in direct orthography-to-phonology conversion linking posterior inferior temporal and intraparietal regions. We then compared activity of these three networks between 16 svPPA patients and the 32 age-matched controls. In svPPA patients, decreased functional connectivity in the ventral semantic network correlated with weak semantic skills, while orthographic network connectivity correlated with pseudoword reading skills. Increased connectivity between the inferior frontal gyrus and the superior portion of the angular gyrus suggested possible adaptive changes.

Our findings support a functional subdivision of the left IPL based on its connectivity to specific language-related regions. Moreover, the unique neuroanatomical and linguistic profile observed in svPPA

provides a compelling model for the functional interplay of these networks, being either up or down regulated in response to disease.

1. INTRODUCTION

The ability to communicate by written or spoken language relies on a sophisticated interplay between the frontal, temporal, and parietal regions that collectively form the language network (Hickok and Poeppel, 2004, 2007; Saur *et al.*, 2008; Ueno *et al.*, 2011; Schwartz *et al.*, 2012). These regions and their neuroanatomical connections are the scaffold on which the three fundamental language domains are built: speech production, semantics, and orthography (Purcell *et al.*, 2011). The involvement of the inferior parietal lobule (IPL) in language processing is also well-established, with references dating back to classic neurological models (Gerstmann, 1971). Far from being a unitary construct, the IPL is a collection of important anatomical, cytoarchitectonic, and functional subdivisions (Nelson *et al.*, 2010; Achal *et al.*, 2016; Wang *et al.*, 2016). Standard parcellations distinguish the angular and supramarginal gyri, but cytoarchtectonic and anatomical atlases define boundaries within and between these two structures with a high degree of variability (Caspers *et al.*, 2006). Previous MR-based functional and structural connectivity studies in healthy controls (HC) have parcellated the IPL (Podzebenko *et al.*, 2005; Nelson *et al.*, 2010; Garcea and Mahon, 2014; Ruschel *et al.*, 2014; Achal *et al.*, 2016; Wang *et al.*, 2016; Wang *et al.*, 2017), but the degree to which heterogeneous IPL sub-regions contribute to specific language processes has yet to be fully determined. Furthermore, few studies have examined connectivity in healthy controls (HC) relative to cognitive and imaging findings in patients with specific behavioral dissociations.

Primary progressive aphasia (PPA) is a clinical syndrome characterized by progressive speech and language deficits caused by selective neurodegeneration of specific language networks (Gorno-Tempini *et*

al., 2004). In the semantic variant PPA (svPPA), atrophy of the anterior temporal lobe (ATL) is associated with impaired semantic memory and difficulties in confrontation naming, word comprehension and reading of words with irregular letter-sound correspondence (surface dyslexia, Binney *et al.* (2016)). The left inferior frontal gyrus (IFG) and IPL are structurally spared in early svPPA, consistent with relatively preserved speech production and phonological processing. However, the angular portion of the IPL has been implicated in different aspects of semantic processing (see Seghier (2013) for a review) and might be functionally disrupted by neurodegeneration of the connected ATL. Furthermore, the spared ability of reading pseudowords and regularization errors in reading exception words suggests preserved posterior temporal and IPL regions that have previously been shown to be involved in word-to-sound mapping (Wilson *et al.*, 2009; Bouhali *et al.*, 2014). Thus, svPPA could provide a lesion model for the selective impairment of IPL-connectivity with semantic regions in conjunction with the relative sparing of connectivity with regions implicated in articulatory and phonological processes.

Resting-state functional MRI (rs-fMRI, Raichle (2006)) serves as the ideal technique to identify functional networks, and has been successfully applied to neurodegenerative diseases (Seeley *et al.*, 2009; Zhou *et al.*, 2010), including PPA (Guo *et al.*, 2013; Mandelli *et al.*, 2016; Collins *et al.*, 2017). Therefore, segmenting IPL subdivisions using the connectivity profile of language-related cortical seeds should elucidate divergent functional connectivity organization in HC and svPPA patients associated with the unique neuroanatomical and linguistic profiles of the disorder.

In this study, we combined seed-based rs-fMRI connectivity and neuropsychological data to (1) identify the brain networks anchored to key regions for speech production, semantics, and orthography; (2) examine how these networks are distributed within the IPL; and (3) investigate how these networks change in response to disease in svPPA and their associations with specific language symptoms. We predicted differential connectivity between unique IPL sub-regions in HC, indicative of anatomically and

functionally distinct language processing networks. We also hypothesized that partially distinct patterns of functional connectivity would be found between HC and svPPA patients, indicating potential markers for clinical phenotype and disease severity.

2. MATERIALS AND METHODS

2.1.Participants

All subjects were right-handed and gave written informed consent for their participation in the study. The experimental procedures were approved by the Committees on Human Research at the University of California San Francisco (UCSF). We studied two groups of participants. The first group of 32 healthy participants (14 males / 18 females; mean age: 64 ± 5.1 years) was used to define language-related functional connectivity networks and to compare statistically with the patient group. Sixteen patients with svPPA (9 males / 7 females; mean age: 62.2 ± 5.9 years) was used to probe the pattern of language-related functional connectivity networks in a neurodegenerative population. All participants were recruited at the Memory and Aging Center (MAC) at the University of California, San Francisco (UCSF, USA) and received comprehensive multidisciplinary evaluations including neurological history and examination, neuropsychological testing, and neuroimaging, as previously described (Gorno-Tempini *et al.*, 2004). A multidisciplinary team diagnosed patients with probable svPPA according to consensus clinical criteria (Gorno-Tempini *et al.*, 2011). Demographic, clinical, and neuropsychological characteristics for patients and healthy age-matched controls are provided in Table 1. To better characterize the patient group in relation to previous studies, we examined global atrophy patterns in svPPA patients using voxel-based morphometry (VBM). Details about the methods are described in the

dedicated section below. We observed the expected pattern of atrophy, involving the bilateral medial and lateral temporal lobes, as well as the bilateral insula (see Figure 1).

Insert Figure 1 about here

Insert Table 1 about here

2.2. Neuroimaging protocol

The neuroimaging protocol for all participants included a high-resolution structural scan for inter-subject registration and atrophy assessment of svPPA patients, as well as an echo-planar imaging (EPI) scan to study resting-state functional connectivity. Participants were instructed to remain still and keep their eyes closed without falling asleep during the acquisition of rs-fMRI data.

Participants were scanned with a Siemens 3 Tesla Trio scanner using a body transmit coil and an 8-channel receive head coil. A T1- weighted 3D Magnetization Prepared Rapid Acquisition Gradient Echo (MPRAGE) was acquired with 160 sagittal slices, echo time (TE)/repetition time (TR)/inversion time (TI) = 2.98/2300/900 ms, flip angle = 9°, 1 x 1 x 1 mm resolution, field of view = 256 x 256 mm, matrix = 256 x 256. For rs-fMRI, 240 T2*-weighted volumes were acquired with an EPI protocol consisting in 36 AC/PC-aligned axial slices acquired in interleaved order. The following other acquisition parameters were utilized: TR/TE = 2000/27 ms, flip angle = 80°, slice thickness = 3 mm with 0.6 mm gap, field of view = 230 x 230 mm, matrix = 92 x 92.

2.3.Voxel-based morphometry (VBM)

Structural MRI data were pre-processed and analyzed using Statistical Parametric Mapping (SPM8, Wellcome Department of Cognitive Neurology, London, UK, http:// www.fil.ion.ucl.ac.uk/spm/software/spm8). For VBM analysis, T1-weighted data were classified as gray matter (GM), white matter (WM), and cerebrospinal fluid (CSF) using the unified segmentation approach (Ashburner and Friston, 2005). GM probability maps were normalized to the Montreal Neurological Institute (MNI) space, modulated by the Jacobian determinant of the deformations derived from the spatial normalization, and smoothed with an isotropic Gaussian kernel of 8 mm full width at half maximum (FWHM). Voxel-based inferential statistic was performed by fitting a general linear model entering age, gender, and total intracranial volume (TIV) as covariates. The statistical map showing GM volume differences between HC and svPPA was thresholded at $p<0.05$, corrected for multiple comparisons using a permutation approach (Wilson *et al.*, 2010). Statistical maps were calculated for 1000 random permutations of subjects' group-identities, and the largest T statistic in each map was used to determine the null distribution of maximum T statistic.

2.4.Rs-fMRI Data Preprocessing

The analysis of functional data was performed using SPM8 and MATLAB (MathWorks, Natick, MA). The first 5 volumes of the acquisition were discarded to allow T_1 equilibrium to be established. Preprocessing and seed-based functional connectivity analyses were performed following an optimized procedure (Weissenbacher *et al.*, 2009). Functional images first were corrected for slice timing and head motion. The mean functional image then was co-registered with the MPRAGE using a rigid body transformation. Rs-fMRI data were normalized to the MNI space using the parameters calculated from the normalization of the MPRAGE, and spatially smoothed with a Gaussian kernel of 5 mm FWHM. Functional data were further corrected for noise using a multiple linear regression against the 6 rigid body realignment parameters, resulting from the head motion correction, the average white matter signals

received from 4 cubic ROIs in the bilateral frontal and parietal WM, the ventricular system signal, and the global signal. The residual data were band-pass filtered (0.0083 - 0.15 Hz).

2.5. Seed-based functional connectivity analysis

Single-subject correlation maps were generated by calculating the correlation coefficient between the average Blood-Oxygen Level Dependent (BOLD) signal time-course from the seed ROIs (described in the next section) and the time course from all other voxels of the brain. Correlation maps were converted to z-scores by Fisher's r-to-z transformation to enable parametric statistical comparisons. Within-subject group analysis for each of the three groups and language networks was performed using a one-sample t-test. The resulting group level connectivity maps were thresholded at $p < 0.05$, corrected for whole-brain family-wise error (FWE) using Gaussian Random Field theory implemented in SPM8. To account for the smaller number of svPPA patients compared to the number of age-matched controls, the group-level maps for the svPPA patients were thresholded voxelwise at $p<0.001$.

2.6. Functional definition of language networks – Seed ROI definition

Language-related functional connectivity networks were determined in healthy controls by calculating group-level connectivity maps for the three language-relevant seeds. These three seed ROIs were defined as 9x9x9 mm boxes, centered at the coordinates derived from language-relevant contrasts in functional activation studies (see Figure 2). The first seed, included for its relevance to speech production, was defined in the left posterior, opercular part of the IFG (opIFG) at the activation peak (MNI coordinates x=-50, y=8, z=23) identified in a previous study by contrasting a phonemic fluency task against semantic and syntactic fluency ones (Heim *et al.*, 2008). This region is highly atrophic in the nonfluent/agrammatic variant of PPA (nfvPPA; (Gorno-Tempini *et al.*, 2004; Mandelli *et al.*, 2016)) and frequently lesioned in cases of post-stroke aphasia (Hillis *et al.*, 2004). Further, brain imaging in healthy,

dyslexic, and deaf adults suggests that this region is implicated in speech production mechanisms, described as "late" phonological or motor speech processes (Brunswick *et al.*, 1999; Bonilha *et al.*, 2006; MacSweeney *et al.*, 2009).

A second seed, potentially relevant for semantic processing, was defined in the left anterior middle temporal gyrus (aMTG) at the activation peak (MNI coordinates x=-60, y=-6, z=-18) identified by contrasting a semantic association task on pairs of famous faces against a perceptual matching task related to pairs of unknown faces (Gesierich *et al.*, 2012). Similar anterior MTG areas have been activated by several other functional neuroimaging studies of semantic processing in healthy subjects (Vandenberghe *et al.*, 1996; Gorno-Tempini *et al.*, 2000; Mechelli *et al.*, 2007; Binder *et al.*, 2009b; Simmons *et al.*, 2010), and this area is consistently atrophic in svPPA (Gorno-Tempini *et al.*, 2004; Patterson *et al.*, 2007b), providing evidence for its critical role in semantic processing. We chose this aMTG region instead of the temporal pole (epicenter of svPPA) due to the extreme atrophy and MRI signal loss of the latter region in these patients. The choice of seeding from a more posterior region to avoid the peak of atrophy in svPPA patients has already been successfully adopted (Guo et al., 2013).

A third seed, potentially relevant for semantic and orthographic processes, was defined in the left posterior ITG (pITG) at the peak (MNI coordinates x=-54, y=-52, z= -10) of a cluster that showed greater activation in controls than in svPPA patients when contrasting a semantic judgment task against a visual judgment task (Mummery *et al.*, 1999). This area has also been defined as the "basal language area" (Burnstine *et al.*, 1990), and its involvement in "multimodal" language processing has been suggested previously (Price and Friston, 1997; Cohen *et al.*, 2004; Fairhall and Caramazza, 2013).

2.7. Functional connectivity changes in the language networks between svPPA and HC

To determine quantitative functional connectivity changes in svPPA patients, we compared single-subject connectivity maps in patients and controls for each of the three language networks. These group comparisons were masked to include only voxels located in the IPL: the supramarginal gyrus (SMG), the intraparietal sulcus (IPS) and the angular gyrus (AG), as defined by the Pickatlas tool (Maldjian *et al.*, 2003) and using the anatomical parcellation of the MNI brain created by Tzourio-Mazoyer and colleagues (Tzourio-Mazoyer *et al.*, 2002). We used a single ROI covering the whole IPL instead of the anatomical networks defined in healthy controls to utilize a larger anatomical mask not restricted only to specific portions of the IPL found in controls. Resulting statistical maps were thresholded first voxelwise at $p<0.01$, and then at the cluster level at $p<0.05$ (FWE small volume corrected for the IPL mask).

To assess whether observed group differences could be explained by underlying grey matter atrophy in either the seed ROI or in the single voxels for which connectivity was estimated, we re-estimated the models, entering the voxel-wise grey matter probability maps and the average grey matter probability in the seed ROI as covariates using the Biological Parametric Mapping toolbox (Casanova *et al.*, 2007). Grey matter probability maps were derived during the segmentation of the structural images in SPM8 (described above) and were smoothed to the same degree as the functional images (Gaussian kernel of 5 mm FWHM).

2.8. Correlation of functional connectivity with cognitive scores

In svPPA patients, we performed correlation analyses between the z-scores of functional connectivity extracted from the IPL sub-regions showing maximum connectivity to each of the seeds and relevant behavioral measures associated with the proposed functional role of the language networks derived from the three seeds. We selected an auditory word recognition test (abbreviated version of Peabody Picture Vocabulary Test, PPVT, Kramer *et al.*, 2003) as a surrogate test of semantic processing.

Pseudoword reading (from the Arizona reading list, Beeson and Rising, 2010), due to its reliance on subword-level analysis of letter strings and their mapping onto plausible phonemes, was selected to test for orthography-to-phonology conversion. As svPPA patients' performance on phonological and motor speech tasks (as detected with selected sub-test of the Western Aphasia Battery, Kertesz, 1982) was at ceiling, we did not test the correlation between connectivity and these behavioral measures. Similarly, we could not perform the same correlation analyses in healthy controls because all behavioral measures were at ceiling in this group. As a control measure, we also included a visuo-spatial processing score that we hypothesized would not associate with any of the functional networks (modified version of Benson figure copy, Kramer et al., 2003). Relationships between the behavioral variables and the extracted z-scores were determined using Spearman partial correlations removing the effect of disease severity in each correlation by controlling for the CDR score.

3. RESULTS

3.1. Definition of language networks in controls and svPPA

In healthy controls, the network resulting from the left opIFG seed included areas in the bilateral opercular and triangular part of the IFG, left middle frontal gyrus, bilateral SMG and IPS, left putamen, left anterior cingulate cortex, and left ITG (Figure 2, Table 2). The network resulting from the left aMTG seed included areas in the bilateral MTG, temporal pole, ITG, precuneus, hippocampus, and parahippocampal gyrus. Additional significant regions were located in the left AG, anterior insula, orbital IFG, anterior and posterior cingulate cortices, as well as in the right middle occipital, and orbital medial frontal gyrus (Figure 2, Table 2). Alternatively, the network resulting from the left pITG seed included areas in the bilateral ITG, left IPS, bilateral triangular IFG, and left precentral gyrus (Figure 2, Table 2).

Insert Figure 2 about here

Insert Table 2 about here

Interestingly, all three networks included peak locations in different portions of the IPL, thereby functionally segmenting the region into distinct areas. The aMTG-seeded network was connected to the inferior portion of the AG (Brodmann area BA 39), while the main IPL targets of the opIFG- and pITG-seeded networks were the SMG (BA40, anterior portion) and IPS (BA 40/7) respectively. The last two networks slightly overlapped in the anterior IPS, whereas the aMTG one did not show any overlap with the remaining networks.

SvPPA patients showed greater spatial representation and overlap of the networks originating from left opIFG and pITG seeds, and reduced extent of the cluster in the AG in the aMTG-seeded network (Figure 3, panel C).

Insert Figure 3 about here

Insert Table 3 about here

3.2. Comparison of IPL functional connectivity between HC and svPPA patients

Compared to age-matched controls, svPPA patients showed stronger connectivity between opIFG and the dorsal-posterior portion of the superior AG (maximum T = 3.97; MNI coordinates: x=-39, y=-64, z=55; cluster extent 4644 mm^3; p = 0.001, FWE corrected, Figure 4, panel A). While this cluster did not overlap with the dorsal network in controls, it did overlap partially with the dorsal network in svPPA (volume of overlap, 459 mm^3), which suggests an expansion of the dorsal network into the AG in svPPA.

Inversely, patients showed decreased connectivity between the aMTG seed and the inferior part of the AG (maximum T = 3.93; MNI coordinates: x=-48, y=-67, z=34; cluster extent 1350 mm3; p = 0.048, FWE corrected) (Figure 4, panel B). This cluster overlapped with the inferior portion of the AG connected to the aMTG via the ventral network in controls and svPPA. There was no significant difference in connectivity between controls and patients in the network connecting the pITG to the IPS.

Insert Figure 4 about here

3.3. Correlations of behavioral measures with functional connectivity

In svPPA patients, we found significant correlations between connectivity scores in the aMTG-to-AG network and PPVT scores (r=0.6, p=0.03), and between connectivity scores in the pITG-to-IPS network and the percentage of correctly read pseudowords (r=0.64, p=0.01). All other correlations were not significant (Figure 5).

Insert Figure 5 about here

4. DISCUSSION

The present study applied whole brain, seed-based connectivity to MRI resting-state data to identify three functionally and anatomically segregated left hemisphere language networks connected to discrete areas within the IPL in healthy controls: a dorsal system involving inferior frontal and supramarginal regions; a ventral network involving anterior middle temporal and angular gyri; and a third linking posterior inferior temporal and intraparietal regions. Our results support a division of the language

system into dorsal and ventral pathways (phonological-articulatory vs. semantics), which map onto distinct sub-regions of the IPL. We propose that the third network, connecting posterior inferior temporal cortex to a region in the intraparietal sulcus, mediates processes related to sub-lexical orthography-to-phonology conversion (further supported by the correlation between functional connectivity within this network and the percentage of correctly read pseudowords in svPPA), supporting an alternate mechanism to process written language in the face of damage to semantic representations. Individuals with svPPA showed spared intrinsic functional connectivity in the orthography-to-phonology conversion network, decreased connectivity in the ventral semantic network, and increased connectivity in the dorsal production network (observed between the inferior frontal gyrus and the superior portion of the angular gyrus), consistent with their language deficits. The up-regulation of the dorsal network suggests a dynamic reorganization of the dorsal pathway in response to degeneration of the anterior temporal lobes.

Inferior frontal - to - Supramarginal network and its role in fluency and phonology

The pars opercularis of the inferior frontal gyrus (opIFG) has been historically described as a key region supporting articulatory-phonological processes, which are preserved in svPPA patients (Gorno-Tempini *et al.*, 2004; Jefferies *et al.*, 2005). Consistently, this network showed normal functional connectivity in individuals with svPPA. Using a left opIFG seed derived from a phonemic fluency task (Heim *et al.*, 2008), we identified a network including fronto-parietal, medial frontal and basal ganglia regions, previously described as the speech production network (Mandelli *et al.*, 2016). Within the parietal cortex, the cluster connected to opIFG was located in the SMG (BA 40) in controls, a region implicated in phonological assembly and phonological-motor integration (Rapcsak *et al.*, 2009; Henry *et al.*, 2012; Price, 2012; Henry *et al.*, 2016). Anatomically, the opIFG is connected to the SMG through white matter fibers of the third portion of the superior longitudinal fasciculus (SLF III, Thiebaut de Schotten *et al.* (2012)). Based on previous data and the known relative sparing of phonological and

articulatory processes in svPPA, we hypothesized that this network sustains fluency in our patients. Furthermore, svPPA subjects showed a larger IPL cluster connected to opIFG, spreading from SMG to the neighboring dorsal and posterior portion of the AG, and overlapping with the pITG network (see Figure 3, panel C). It could be speculated that svPPA patients make increased use of IFG-mediated verbalization and phonological strategies during language tasks. Therefore, the increase in connectivity between opIFG and the dorsal-posterior AG may reflect an enhancement of the dorsal articulatory-phonological system, with recruitment of a larger cortical hub. Decreased connectivity of the ventral semantic network would result in increased overlap and connectivity between orthographical-phonological and motor speech systems, and a larger AG cortical hub. It is a clinical observation that when patients with mild svPPA cannot name an object, they often produce the name of the first letter of the word and even a few phonemes.

Anterior middle temporal - to - angular network and its role in semantics

The anterior middle temporal gyrus (aMTG), located posteriorly to svPPA patients' disease epicenter in the anterior temporal lobe, has been associated with semantic processing in this disorder and in healthy subjects (Patterson *et al.*, 2007a). In our study, the inferior AG (BA 39) emerged as the IPL sub-region most strongly linked to the aMTG. Anatomical studies in human and non-human primates show the existence of structural connections between these regions through fibers of the middle longitudinal fasciculus (Burks *et al.*, 2017). This ventral temporo-parietal language network includes medial temporal and posterior cingulate regions, corresponding to portions of the default network (DMN); the activation of the DMN in task-free functional studies is well-established and has been associated with several cognitive processes (Greicius *et al.*, 2003). This ventral system also has been consistently implicated in semantic processing in fMRI activation studies of healthy adults (see meta-analysis by Binder *et al.*, 2009a), thus establishing its role in language comprehension and semantics (Gorno-Tempini

et al., 1998; Binder *et al.*, 2003; Mechelli *et al.*, 2007; Seghier *et al.*, 2010; Gesierich *et al.*, 2011). However, the precise role of the AG hub is still controversial. Cognitive models suggest the AG's involvement in the retrieval or rapid combination of conceptual information, rather than formation and storage of conceptual representations (Jefferies and Lambon Ralph, 2006; Binder *et al.*, 2009a). As the AG is not significantly atrophied in our and other groups of svPPA patients, the observed functional connectivity alteration in the AG is likely the result of a functional diaschisis with the degenerating aMTG. This finding highlights the network-wide and large-scale consequences of focal neurodegeneration (Guo *et al.*, 2013; Collins *et al.*, 2017). Therefore, the profound single word comprehension and semantic deficit in svPPA are likely due to, not only the atrophy of the aMTG, but also the dysfunction of the whole semantic network (Mummery *et al.*, 1999). Consistently, strength of connectivity in this ventral network correlated with deficits in the number of recognized words as measured by the Peabody Picture Vocabulary Test in svPPA, thus further supporting the role of this network in semantic processing.

Posterior inferior temporal - to - intraparietal network and its role in orthography and attention

The posterior ITG (pITG) is a key region that helps to link visual to linguistic processes in reading and naming studies. Atrophy in svPPA starts from the temporal lobe and progresses posteriorly, and thus, this region usually is spared until the late stages of the disorder. The functional network derived from seeding in the pITG included areas in the bilateral ITG, left intraparietal sulcus (IPS), bilateral triangular IFG, and left precentral gyrus. Within the IPL, the region that connected to pITG primarily was centered in the IPS (BA 40), lying posteriorly to the SMG fluency hub and dorsally to the AG semantic hub (see Figure 2). Anatomically, the IPS is connected to the pITG through temporo-parietal white matter fibers of the posterior segment of the SLF (Thiebaut de Schotten *et al.*, 2012). The intrinsic connectivity pattern within the network in svPPA did not differ from that of healthy controls. This network involves regions

commonly associated with both multimodal and orthographic language processes (Price and Friston, 1997; Cohen *et al.*, 2004; Purcell *et al.*, 2011; Fairhall and Caramazza, 2013). Similar connectivity patterns have been observed in studies investigating functional connectivity using seeds in the so-called "visual word form area" (Koyama *et al.*, 2010; Zhao *et al.*, 2011; Vogel *et al.*, 2012). However, the specific role of this network in the multi-component reading process is still disputed. Individuals with svPPA typically show surface dyslexia, characterized by impaired exception word reading and relatively spared pseudo-word reading. A previous task-based fMRI study investigating the neural basis of reading in svPPA (Wilson *et al.*, 2009) suggested that the IPS may be involved in sub-lexical reading. This area was activated in controls and svPPA patients when reading pseudowords, which necessitates the application of sub-lexical orthography-to-phonology transformations. Additionally, the same region showed greater activation when svPPA patients made "over-regularization errors" on words with irregular spelling-to-sound correspondences (irregularly-spelled words). This type of reading error has been described as an improper application of sub-lexical reading processes in the event of a failure to retrieve item-specific "semantic" information (Patterson and Hodges, 1992). In this study, connectivity metrics in this network correlated with patients' pseudoword reading scores, providing additional evidence for its role in sub-lexical reading. This posterior network is preferentially engaged when a visually-presented word is not recognized as a single unit, either because of its non-lexical status (i.e., pseudowords) or because damage within the semantic hub impairs access to the associated word-specific pattern (as occurs with exception words in svPPA). The IPS may provide the attentional resources needed to scan the visually-represented letter string and segment it into plausible graphemes for subsequent conversion into the relevant phonemes. The finding that the IPS is often activated in spatial and feature-based attention tasks (Corbetta and Shulman, 2002; Vogel *et al.*, 2012) favors this hypothesis.

4.1. Limitations

The current work relies on the comparison of functional connectivity profiles in healthy control with a single variant of PPA. Further studies are needed to localize distinct and shared patterns of connectivity in the three variants of PPA (logopenic vs. non-fluent vs. semantics) and to fully characterize the differential involvement of the IPL in PPA. Moreover, further work is needed to investigate the behavioral relevance of the reorganization of the dorsal pathway observed in svPPA, and probe its potential for therapeutic purposes.

4.2. Conclusion

Our study identifies three segregated resting-state functional language networks anchored to seeds previously shown to be involved in speech production, semantics, and orthography. These networks are connected to discrete left IPL sub-regions, supporting this region's multidimensional role in language processing. Furthermore, our data provide evidence that changes in functional connectivity of this region reflect not only the behavioral impairments observed in svPPA, but also possible neural adaptations. The unique neuroanatomical and linguistic profile observed in svPPA provides a compelling model for the functional and dynamic interplay of these networks, reflecting up-or down-regulation in response to disease. Furthermore, identifying functional language networks in specific disease profiles characterized by loss and sparing of such functions, as seen in svPPA, represents a powerful model to study the neurobiology of language.

5. ACKNOWLEDGMENTS

The authors thank the patients and their families for the time and effort they dedicated to the research. The authors declare no competing financial interests.

6. FUNDING

The study was supported by grants from the National Institutes of Health (NINDS R01NS050915, NIDCD K24DC015544, NIDCD R03DC013403, NIDCD F32DC009145, NIA U01AG052943, NIA P50AG023501, NIA P01AG019724, NIA R01AG038791, NINDS U54NS092089 Alzheimer's Disease Research Center of California (03-75271 DHS/ADP/ARCC); Larry L. Hillblom Foundation; John Douglas French Alzheimer's Foundation; Koret Family Foundation; Consortium for Frontotemporal Dementia Research; and McBean Family Foundation.

7. REFERENCES

Achal S, Hoeft F, Bray S. Individual Differences in Adult Reading Are Associated with Left Temporo-parietal to Dorsal Striatal Functional Connectivity. Cereb Cortex 2016; 26(10): 4069-81.

Ashburner J, Friston KJ. Unified segmentation. Neuroimage 2005; 26(3): 839-51.

Binder JR, Desai RH, Graves WW, Conant LL. Where is the semantic system? A critical review and meta-analysis of 120 functional neuroimaging studies. Cerebral Cortex 2009a; 19(12): 2767-96.

Binder JR, Desai RH, Graves WW, Conant LL. Where is the semantic system? A critical review and meta-analysis of 120 functional neuroimaging studies. Cereb Cortex 2009b; 19(12): 2767-96.

Binder JR, McKiernan KA, Parsons ME, Westbury CF, Possing ET, Kaufman JN, *et al.* Neural correlates of lexical access during visual word recognition. J Cogn Neurosci 2003; 15(3): 372-93.

Binney RJ, Henry ML, Babiak M, Pressman PS, Santos-Santos MA, Narvid J, *et al.* Reading words and other people: A comparison of exception word, familiar face and affect processing in the left and right temporal variants of primary progressive aphasia. Cortex 2016; 82: 147-63.

Bonilha L, Moser D, Rorden C, Baylis GC, Fridriksson J. Speech apraxia without oral apraxia: can normal brain function explain the physiopathology? Neuroreport 2006; 17(10): 1027-31.

Bouhali F, Thiebaut de Schotten M, Pinel P, Poupon C, Mangin JF, Dehaene S, *et al.* Anatomical connections of the visual word form area. J Neurosci 2014; 34(46): 15402-14.

Brunswick N, McCrory E, Price CJ, Frith CD, Frith U. Explicit and implicit processing of words and pseudowords by adult developmental dyslexics: A search for Wernicke's Wortschatz? Brain 1999; 122 (Pt 10): 1901-17.

Burks JD, Boettcher LB, Conner AK, Glenn CA, Bonney PA, Baker CM, *et al.* White matter connections of the inferior parietal lobule: A study of surgical anatomy. Brain Behav 2017; 7(4): e00640.

Burnstine TH, Lesser RP, Hart J, Jr., Uematsu S, Zinreich SJ, Krauss GL, *et al.* Characterization of the basal temporal language area in patients with left temporal lobe epilepsy. Neurology 1990; 40(6): 966-70.

Casanova R, Srikanth R, Baer A, Laurienti PJ, Burdette JH, Hayasaka S, *et al.* Biological parametric mapping: A statistical toolbox for multimodality brain image analysis. Neuroimage 2007; 34(1): 137-43.

Caspers S, Geyer S, Schleicher A, Mohlberg H, Amunts K, Zilles K. The human inferior parietal cortex: cytoarchitectonic parcellation and interindividual variability. Neuroimage 2006; 33(2): 430-48.

Cohen L, Jobert A, Le Bihan D, Dehaene S. Distinct unimodal and multimodal regions for word processing in the left temporal cortex. Neuroimage 2004; 23(4): 1256-70.

Collins JA, Montal V, Hochberg D, Quimby M, Mandelli ML, Makris N, *et al.* Focal temporal pole atrophy and network degeneration in semantic variant primary progressive aphasia. Brain 2017; 140(2): 457-71.

Corbetta M, Shulman GL. Control of goal-directed and stimulus-driven attention in the brain. Nat Rev Neurosci 2002; 3(3): 201-15.

Fairhall SL, Caramazza A. Brain regions that represent amodal conceptual knowledge. J Neurosci 2013; 33(25): 10552-8.

Garcea FE, Mahon BZ. Parcellation of left parietal tool representations by functional connectivity. Neuropsychologia 2014; 60: 131-43.

Gesierich B, Jovicich J, Riello M, Adriani M, Monti A, Brentari V, *et al.* Distinct Neural Substrates for Semantic Knowledge and Naming in the Temporoparietal Network. Cereb Cortex 2011.

Gesierich B, Jovicich J, Riello M, Adriani M, Monti A, Brentari V, *et al.* Distinct neural substrates for semantic knowledge and naming in the temporoparietal network. Cereb Cortex 2012; 22(10): 2217-26.

Gorno-Tempini ML, Cipolotti L, Price CJ. Category differences in brain activation studies: where do they come from? Proc Biol Sci 2000; 267(1449): 1253-8.

Gorno-Tempini ML, Dronkers NF, Rankin KP, Ogar JM, Phengrasamy L, Rosen HJ, *et al.* Cognition and anatomy in three variants of primary progressive aphasia. Ann Neurol 2004; 55(3): 335-46.

Gorno-Tempini ML, Hillis AE, Weintraub S, Kertesz A, Mendez M, Cappa SF, *et al.* Classification of primary progressive aphasia and its variants. Neurology 2011; 76(11): 1006-14.

Gorno-Tempini ML, Price CJ, Josephs O, Vandenberghe R, Cappa SF, Kapur N, *et al.* The neural systems sustaining face and proper-name processing. Brain 1998; 121 (Pt 11): 2103-18.

Guo CC, Gorno-Tempini ML, Gesierich B, Henry M, Trujillo A, Shany-Ur T, *et al.* Anterior temporal lobe degeneration produces widespread network-driven dysfunction. Brain 2013; 136(Pt 10): 2979-91.

Greicius MD, Krasnow B, Reiss AL, Menon V. Functional connectivity in the resting brain: a network analysis of the default mode hypothesis. Proc Natl Acad Sci U S A 2003; 100(1): 253-8.

Heim S, Eickhoff SB, Amunts K. Specialisation in Broca's region for semantic, phonological, and syntactic fluency? Neuroimage 2008; 40(3): 1362-8.

Henry ML, Beeson PM, Alexander GE, Rapcsak SZ. Written language impairments in primary progressive aphasia: a reflection of damage to central semantic and phonological processes. J Cogn Neurosci 2012; 24(2): 261-75.

Henry ML, Wilson SM, Babiak MC, Mandelli ML, Beeson PM, Miller ZA, *et al.* Phonological Processing in Primary Progressive Aphasia. J Cogn Neurosci 2016; 28(2): 210-22.

Hickok G, Poeppel D. Dorsal and ventral streams: a framework for understanding aspects of the functional anatomy of language. Cognition 2004; 92(1-2): 67-99.

Hickok G, Poeppel D. The cortical organization of speech processing. Nat Rev Neurosci 2007; 8(5): 393-402.

Hillis AE, Work M, Barker PB, Jacobs MA, Breese EL, Maurer K. Re-examining the brain regions crucial for orchestrating speech articulation. Brain 2004; 127(Pt 7): 1479-87.

Jefferies E, Jones RW, Bateman D, Ralph MA. A semantic contribution to nonword recall? Evidence for intact phonological processes in semantic dementia. Cogn Neuropsychol 2005; 22(2): 183-212.

Jefferies E, Lambon Ralph MA. Semantic impairment in stroke aphasia versus semantic dementia: a case-series comparison. Brain 2006; 129(Pt 8): 2132-47.

Kertesz, A. Western aphasia battery test manual. New York: Grune & Stratton, 1982.

Koyama MS, Kelly C, Shehzad Z, Penesetti D, Castellanos FX, Milham MP. Reading networks at rest. Cereb Cortex 2010; 20(11): 2549-59.

Kramer JH, Jurik J, Sha SJ, Rankin KP, Rosen HJ, Johnson JK, *et al.* Distinctive neuropsychological patterns in frontotemporal dementia, semantic dementia, and Alzheimer disease. Cogn Behav Neurol 2003; 16(4): 211-8.

MacSweeney M, Brammer MJ, Waters D, Goswami U. Enhanced activation of the left inferior frontal gyrus in deaf and dyslexic adults during rhyming. Brain 2009; 132(Pt 7): 1928-40.

Maldjian JA, Laurienti PJ, Kraft RA, Burdette JH. An automated method for neuroanatomic and cytoarchitectonic atlas-based interrogation of fMRI data sets. Neuroimage 2003; 19(3): 1233-9.

Mandelli ML, Vilaplana E, Brown JA, Hubbard HI, Binney RJ, Attygalle S, *et al.* Healthy brain connectivity predicts atrophy progression in non-fluent variant of primary progressive aphasia. Brain 2016; 139(Pt 10): 2778-91.

Mechelli A, Josephs O, Lambon Ralph MA, McClelland JL, Price CJ. Dissociating stimulus-driven semantic and phonological effect during reading and naming. Hum Brain Mapp 2007; 28(3): 205-17.

Mummery CJ, Patterson K, Wise RJ, Vandenberghe R, Price CJ, Hodges JR. Disrupted temporal lobe connections in semantic dementia. Brain 1999; 122 (Pt 1): 61-73.

Nelson SM, Cohen AL, Power JD, Wig GS, Miezin FM, Wheeler ME, *et al.* A parcellation scheme for human left lateral parietal cortex. Neuron 2010; 67(1): 156-70.

Patterson K, Hodges JR. Deterioration of word meaning: implications for reading. Neuropsychologia 1992; 30(12): 1025-40.

Patterson K, Nestor PJ, Rogers TT. Where do you know what you know? The representation of semantic knowledge in the human brain. Nature reviews Neuroscience 2007a; 8(12): 976-87.

Patterson K, Nestor PJ, Rogers TT. Where do you know what you know? The representation of semantic knowledge in the human brain. Nat Rev Neurosci 2007b; 8(12): 976-87.

Podzebenko K, Egan GF, Watson JD. Real and imaginary rotary motion processing: functional parcellation of the human parietal lobe revealed by fMRI. J Cogn Neurosci 2005; 17(1): 24-36.

Price CJ. A review and synthesis of the first 20 years of PET and fMRI studies of heard speech, spoken language and reading. Neuroimage 2012; 62(2): 816-47.

Price CJ, Friston KJ. The temporal dynamics of reading: a PET study. Proc Biol Sci 1997; 264(1389): 1785-91.

Purcell JJ, Turkeltaub PE, Eden GF, Rapp B. Examining the central and peripheral processes of written word production through meta-analysis. Front Psychol 2011; 2: 239.

Raichle ME. Neuroscience. The brain's dark energy. Science 2006; 314(5803): 1249-50.

Rapcsak SZ, Beeson PM, Henry ML, Leyden A, Kim E, Rising K, *et al.* Phonological dyslexia and dysgraphia: cognitive mechanisms and neural substrates. Cortex 2009; 45(5): 575-91.

Ruschel M, Knosche TR, Friederici AD, Turner R, Geyer S, Anwander A. Connectivity architecture and subdivision of the human inferior parietal cortex revealed by diffusion MRI. Cereb Cortex 2014; 24(9): 2436-48.

Saur D, Kreher BW, Schnell S, Kummerer D, Kellmeyer P, Vry MS, *et al.* Ventral and dorsal pathways for language. Proc Natl Acad Sci U S A 2008; 105(46): 18035-40.

Schwartz MF, Faseyitan O, Kim J, Coslett HB. The dorsal stream contribution to phonological retrieval in object naming. Brain 2012; 135(Pt 12): 3799-814.

Seeley WW, Crawford RK, Zhou J, Miller BL, Greicius MD. Neurodegenerative diseases target large-scale human brain networks. Neuron 2009; 62(1): 42-52.

Seghier ML. The angular gyrus: multiple functions and multiple subdivisions. Neuroscientist 2013; 19(1): 43-61.

Seghier ML, Fagan E, Price CJ. Functional subdivisions in the left angular gyrus where the semantic system meets and diverges from the default network. Journal of Neuroscience 2010; 30(50): 16809-17.

Simmons WK, Reddish M, Bellgowan PS, Martin A. The selectivity and functional connectivity of the anterior temporal lobes. Cereb Cortex 2010; 20(4): 813-25.

Thiebaut de Schotten M, Dell'Acqua F, Valabregue R, Catani M. Monkey to human comparative anatomy of the frontal lobe association tracts. Cortex 2012; 48(1): 82-96.

Tzourio-Mazoyer N, Landeau B, Papathanassiou D, Crivello F, Etard O, Delcroix N, *et al.* Automated anatomical labeling of activations in SPM using a macroscopic anatomical parcellation of the MNI MRI single-subject brain. Neuroimage 2002; 15(1): 273-89.

Ueno T, Saito S, Rogers TT, Lambon Ralph MA. Lichtheim 2: synthesizing aphasia and the neural basis of language in a neurocomputational model of the dual dorsal-ventral language pathways. Neuron 2011; 72(2): 385-96.

Vandenberghe R, Price C, Wise R, Josephs O, Frackowiak RS. Functional anatomy of a common semantic system for words and pictures. Nature 1996; 383(6597): 254-6.

Vogel AC, Miezin FM, Petersen SE, Schlaggar BL. The putative visual word form area is functionally connected to the dorsal attention network. Cereb Cortex 2012; 22(3): 537-49.

Wang J, Xie S, Guo X, Becker B, Fox PT, Eickhoff SB, *et al.* Correspondent Functional Topography of the Human Left Inferior Parietal Lobule at Rest and Under Task Revealed Using Resting-State fMRI and Coactivation Based Parcellation. Hum Brain Mapp 2017; 38(3): 1659-75.

Wang J, Zhang J, Rong M, Wei X, Zheng D, Fox PT, *et al.* Functional topography of the right inferior parietal lobule structured by anatomical connectivity profiles. Hum Brain Mapp 2016; 37(12): 4316-32.

Weissenbacher A, Kasess C, Gerstl F, Lanzenberger R, Moser E, Windischberger C. Correlations and anticorrelations in resting-state functional connectivity MRI: a quantitative comparison of preprocessing strategies. Neuroimage 2009; 47(4): 1408-16.

Wilson SM, Brambati SM, Henry RG, Handwerker DA, Agosta F, Miller BL, *et al.* The neural basis of surface dyslexia in semantic dementia. Brain 2009; 132(Pt 1): 71-86.

Wilson SM, Henry ML, Besbris M, Ogar JM, Dronkers NF, Jarrold W, *et al.* Connected speech production in three variants of primary progressive aphasia. Brain 2010; 133(Pt 7): 2069-88.

Zhao J, Liu J, Li J, Liang J, Feng L, Ai L, *et al.* Intrinsically organized network for word processing during the resting state. Neurosci Lett 2011; 487(1): 27-31.

Zhou J, Greicius MD, Gennatas ED, Growdon ME, Jang JY, Rabinovici GD, *et al.* Divergent network connectivity changes in behavioural variant frontotemporal dementia and Alzheimer's disease. Brain 2010; 133(Pt 5): 1352-67.

8. FIGURE LEGENDS

Figure 1. Atrophy pattern in the svPPA patients. Map was thresholded at p(FWE)<0.05 using a permutation approach, and shown on a rendered surface of the Montreal Neurological Institute (MNI) template. Colorbar represents T-score.

Figure 2. Functional connectivity networks in healthy controls (p<0.05, FWE corrected; height threshold T=5.88). Right upper panel shows location of the three seeds in the left opIFG (red), left aMTG (green), and the left pITG (blue). Arrows indicate the network revealed for each of these seeds. Left hemispheres are shown.

Figure 3. The three language networks in the two subject groups. Networks are colored according to the colors of the seeds shown in Figure 2: opIFG network (red); aMTG network (green); pITG network (blue). Maps in HC, (panel A) are thresholded at p<0.05, FWE corrected (height threshold T=5.88), and voxel-wise at p<0.001 for the svPPA patients (height threshold T=3.73, panel B). A surface rendering as well as coronal IPL sections are shown for the left hemisphere.

Figure 4. Comparison of functional connectivity between svPPA patients and healthy controls. SvPPA patients showed stronger connectivity with the opIFG seed in the upper part of the angular gyrus

(panel A). Decreased connectivity with the aMTG seed was found in the lower part of the angular gyrus (panel B) instead. Results were thresholded voxel-wise at $p<0.01$, and corrected for family-wise error rate $p<0.05$ at cluster level. Seeds are shown as red (opIFG seed) and green (aMTG seed) boxes on the surface rendering of the left hemisphere. Coronal IPL sections are shown for the left hemisphere.

Figure 5. Functional connectivity-behavioral correlations. Panel A highlights the dissociation of the language networks by showing that patients' performance only on the PPVT score significantly correlated with functional connectivity in the aMTG-to-AG network, while performance on Pseudoword reading correlated with pITG-to-IPS connectivity. The horizontal axis displays the Spearman correlation coefficients, and the vertical axis lists the names of the behavioral measures. Panel B shows the scatter plots of the significant correlations. The % of correct items in the behavioral scores (horizontal axes) were plotted against the residual of the functional connectivity scores after removing the effect of disease severity through the CDR score.

Table 1. Demographic, clinical, and neuropsychological characteristics of patients and controls.

Variables	svPPA			Controls (HC2)			
Demographics							
Age	62.5	±	5.9	64.0	±	5.1	
Sex (M/F)	9/7			14/18			
Education (years)	17.0	±	2.6	17.6	±	2.0	
Clinical							
Mini Mental Status Examination (30)	26.5	±	2.2	29.4	±	0.8	*
Clinical Dementia Rating	0.7	±	0.4	0	±	0	*
Clinical Dementia Rating (sum of boxes)	4.1	±	2.9	0.0	±	0.1	*
Age at disease onset	55.9	±	7.3	N/A	±	N/A	
Years from first symptoms	6.0	±	3.8	N/A	±	N/A	
Language production							
Confrontation naming (BNT, 15)	6.4	±	4.0	14.5	±	0.6	*
Phonemic fluency (D words in 1 min)	7.3	±	3.1	15.0	±	4.0	*
Semantic fluency (Animals in 1 min)	8.7	±	3.3	24.1	±	4.1	*
Speech fluency (WAB, 10)	8.9	±	0.7	10.0	±	0.0	◤
Apraxia of speech rating (MSE, 7)	0.0	±	0.0	0.0	±	0.0	
Dysarthria rating (MSE, 7)	0.0	±	0.0	0.0	±	0.0	
Repetition (WAB, 100)	92.8	±	7.0	99.5	±	0.9	◤
Language comprehension							
Auditory word recognition (PPVT, 16)	10.0	±	4.2	15.9	±	0.4	*
Sequential commands (WAB, 80)	76.5	±	7.2	80.0	±	0.0	◤
Semantic knowledge (PPT-P, 52)	42.4	±	7.2	51.8	±	0.4	◤
Reading							
Regular words (100)	96.8	±	6.0	100.0	±	0.0	◤
Exceptional words (100)	87.0	±	16.3	99.8	±	0.6	◤
Pseudo-words (100)	90.7	±	12.2	97.8	±	3.6	◤

Visuospatial function							
Modified Rey–Osterrieth copy (17)	15.5	±	1.0	15.0	±	1.1	
Visual memory							
Modified Rey–Osterrieth delay (17)	6.2	±	4.8	12.5	±	2.0	*
Verbal memory							
CVLT-MS trials 1–4 (40)	19.3	±	6.4	28.7	±	3.1	◤
CVLT-MS 30 s free recall (10)	3.9	±	2.5	7.9	±	1.6	◤
CVLT-MS 10 min free recall (10)	2.3	±	2.4	7.3	±	1.6	◤
Executive function							
Digit span backwards	4.8	±	0.8	5.7	±	1.1	*
Modified trails (lines per minute)	21.0	±	10.0	37.7	±	10.2	*
Calculation (5)	4.6	±	0.5	4.8	±	0.4	

*Values are means ±SD. * Significantly impaired relative to controls, $p < 0.05$. □ Since the present control group was not tested on these variables, we used data from Gorno-Tempini et al. (2004) and an independent group of 17 healthy participants to test differences in these scores between a control population and the svPPA patients enrolled in this study. BNT, Boston Naming Test; WAB, Western Aphasia Battery; MSE, Motor Speech Evaluation; PPVT, Peabody Picture Vocabulary Test; PPT-P, Pyramids and Palm Trees-Pictures; CVLT-MS, California Verbal Learning Test-Mental Status. See Kramer et al. (2003) for detailed description of neuropsychological testing procedures and Gorno-Tempini et al. (2004) for detailed description of language testing procedures.*

Table 2: Functional connectivity maps for the three language related seeds in HC1.

Seed	Brain area	MNI coordinates			Extent (mm^3)	P (FWE)	Max T
		x	y	z			
opIFG	Left inferior frontal opercular	-51	9	21	14256	<0.001	31.1
	Left inferior frontal triangular	*-42*	*36*	*15*			*9.23*
	Left middle frontal orbital	*-42*	*48*	*-9*			*7.91*
	Right inferior frontal opercular	51	9	24	6291	<0.001	12.85
	Left inferior parietal	-54	-30	45	13824	<0.001	12.64
	Left supramarginal	*-60*	*-27*	*36*			*11.35*

	Left intraparietal	*-45*	*-45*	*54*			*8.18*	*Note:*
	Left putamen	-27	15	3	5724	<0.001	10.59	*P*
	Left pallidum	*-21*	*0*	*3*			*9.36*	
	Right supramarginal	60	-15	27	6183	<0.001	10.29	*values*
	Right supramarginal	*51*	*-33*	*42*			*8.71*	
	Right inferior frontal triangular	48	39	6	2268	<0.001	10.21	*(P)*
	Left superior parietal	-21	-60	51	351	<0.001	8.72	
	Right insula	39	0	3	648	<0.001	8.16	*and*
	Left anterior cingulum	3	3	27	324	0.003	7.7	
	Left inferior temporal	-54	-57	-6	459	0.004	7.53	*maxim*
aMTG	Left middle temporal	-60	-9	-18	26001	<0.001	29.1	*um T*
	Left anterior insula	*-30*	*3*	*-12*			*13.58*	*statisti*
	Left inferior temporal	*-39*	*6*	*-33*			*12.74*	
	Right middle temporal	60	0	-21	13554	<0.001	15.79	*cs*
	Right superior temporal pole	*39*	*15*	*-30*			*12.43*	
	Right middle temporal pole	*48*	*12*	*-24*			*11.99*	*(Max*
	Right middle occipital	48	-63	24	3591	<0.001	14.45	
	Left precuneus	-6	-54	36	17334	<0.001	12.65	*T) are*
	Right precuneus	*0*	*-63*	*21*			*12.41*	
	Left precuneus	*-6*	*-51*	*9*			*11.07*	*report*
	Left angular	-45	-66	27	6912	<0.001	12.31	
	Right parahippocampal	24	-15	-21	3105	<0.001	11.83	*ed for*
	Left inferior frontal orbital	-45	30	-9	702	<0.001	10.84	
	Right medial frontal orbital	6	54	-9	5265	<0.001	9.74	*the*
	Right rectus	*6*	*33*	*-18*			*8.06*	*peak*
	Left anterior cingulum	*-6*	*45*	*6*			*7.51*	
								voxel
pITG	Left inferior temporal	-54	-51	-15	9531	<0.001	33.08	
	Left inferior temporal	*-60*	*-36*	*-21*			*10.29*	*of*
	Left intraparietal	-33	-51	36	6426	<0.001	11.5	
	Left intraparietal	*-42*	*-48*	*45*			*11.43*	*each*
	Right inferior temporal	63	-51	-12	1863	<0.001	10.27	
	Right inferior frontal triangular	51	36	15	324	<0.001	8.65	*cluster*
	Left precentral	-48	12	33	567	<0.001	8.34	
	Left inferior frontal triangular	-42	36	15	864	<0.001	8.28	*. P*

values were controlled for FWE. For single clusters, which cover larger cortical areas or extend into different areas of the brain, the local maxima in these additional areas are indicated in italics.

Figure 1

Click here to download high resolution image

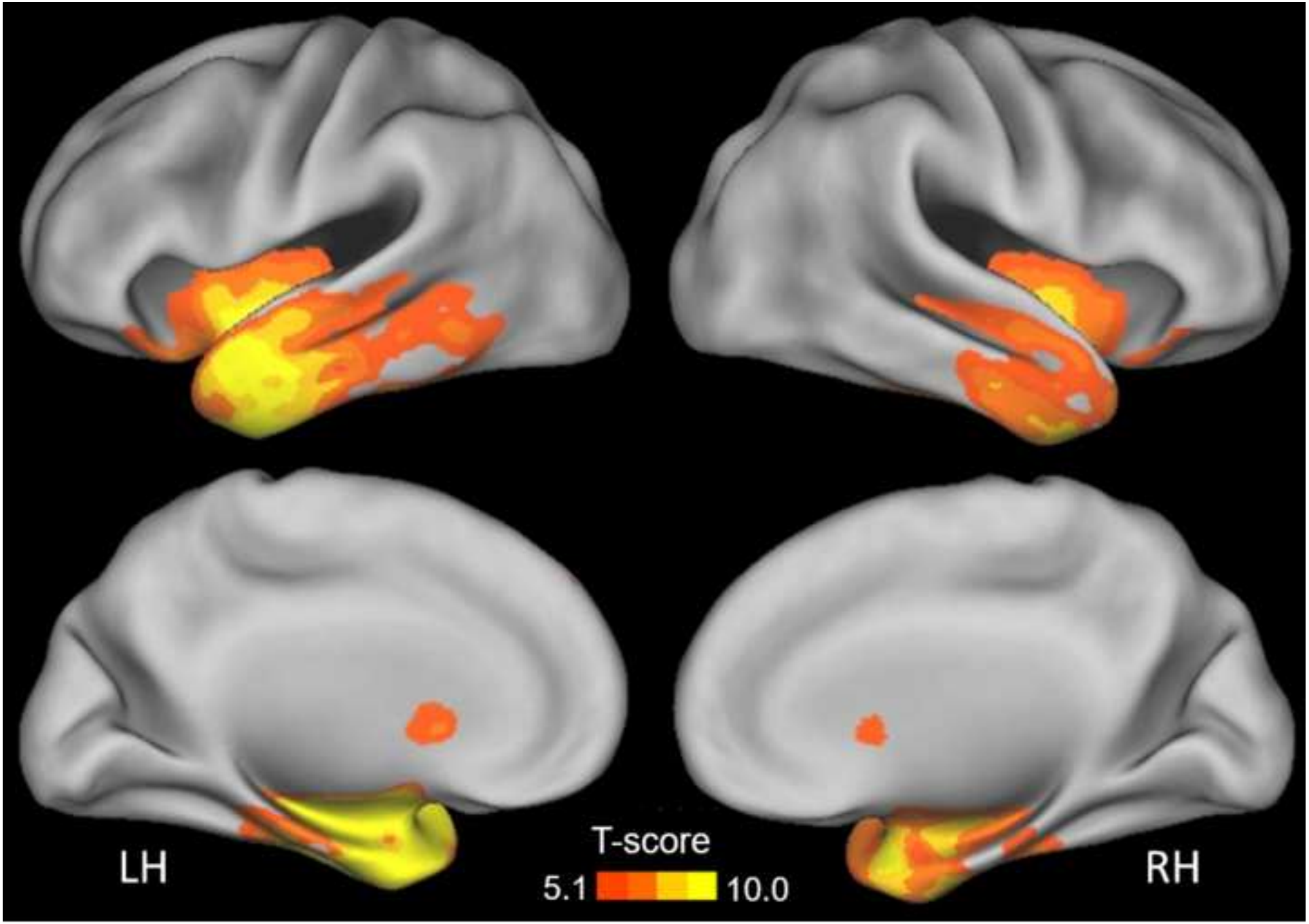

Figure 2

Click here to download high resolution image

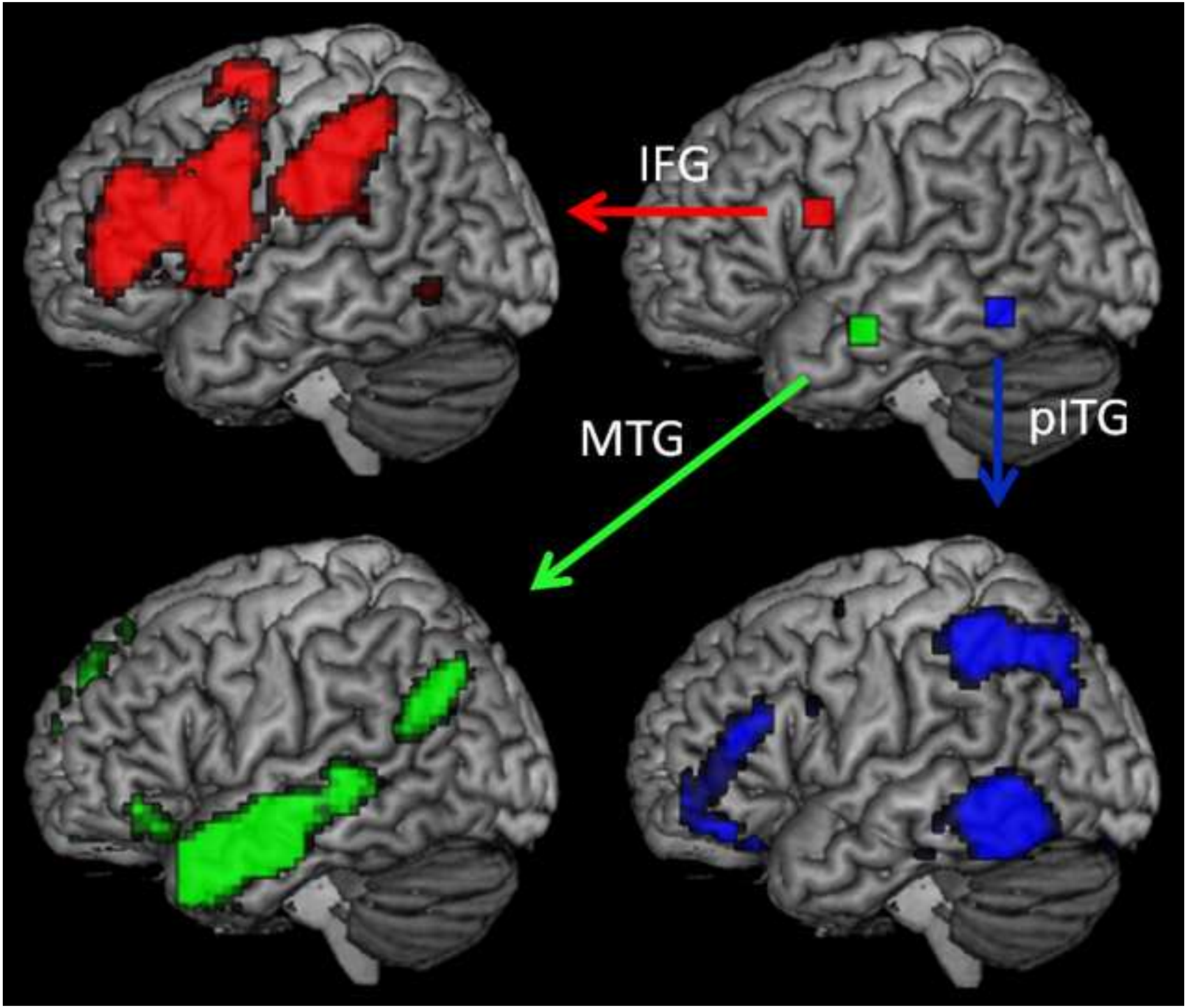

Figure 3

Click here to download high resolution image

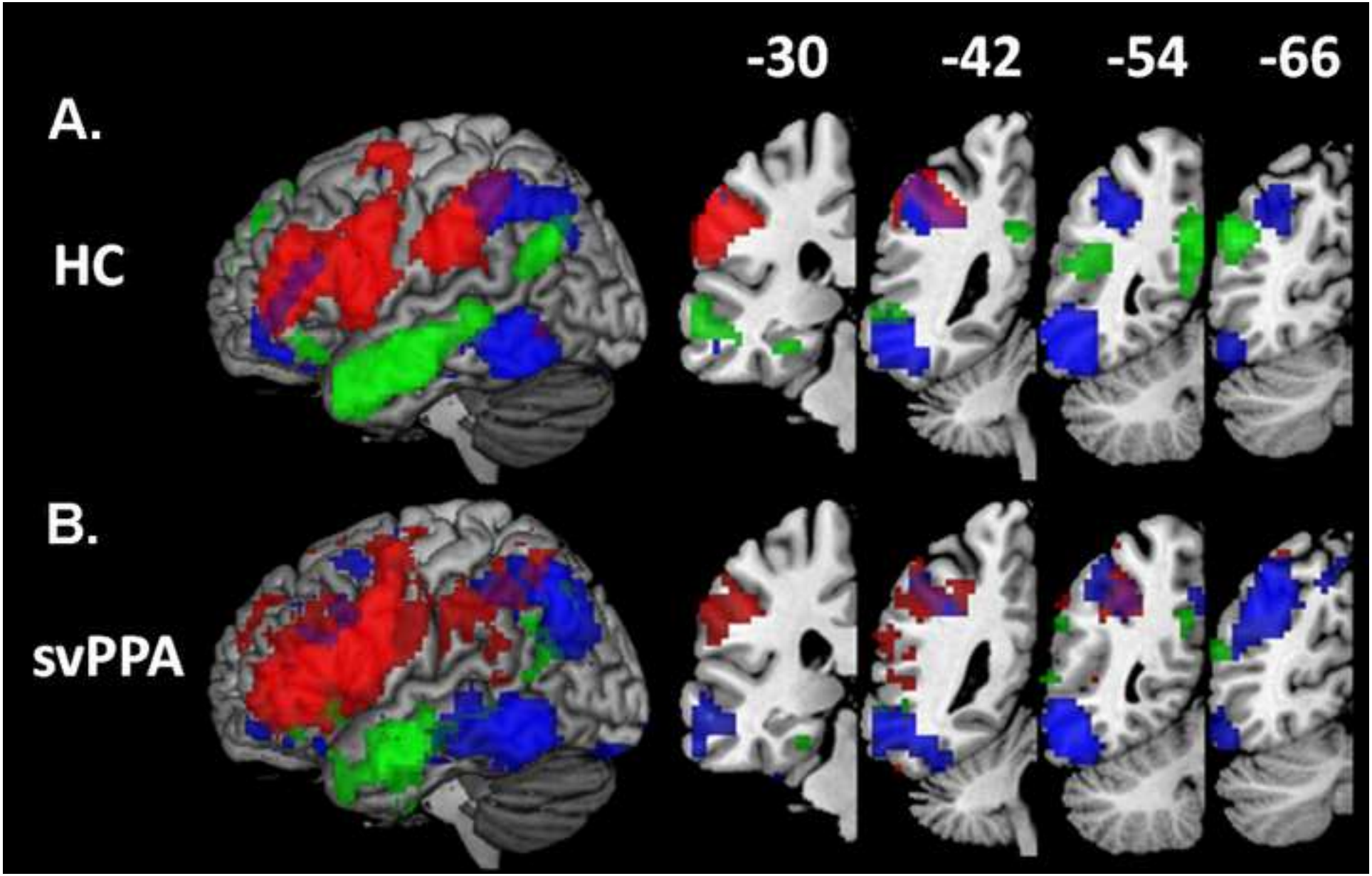

Figure 4

Click here to download high resolution image

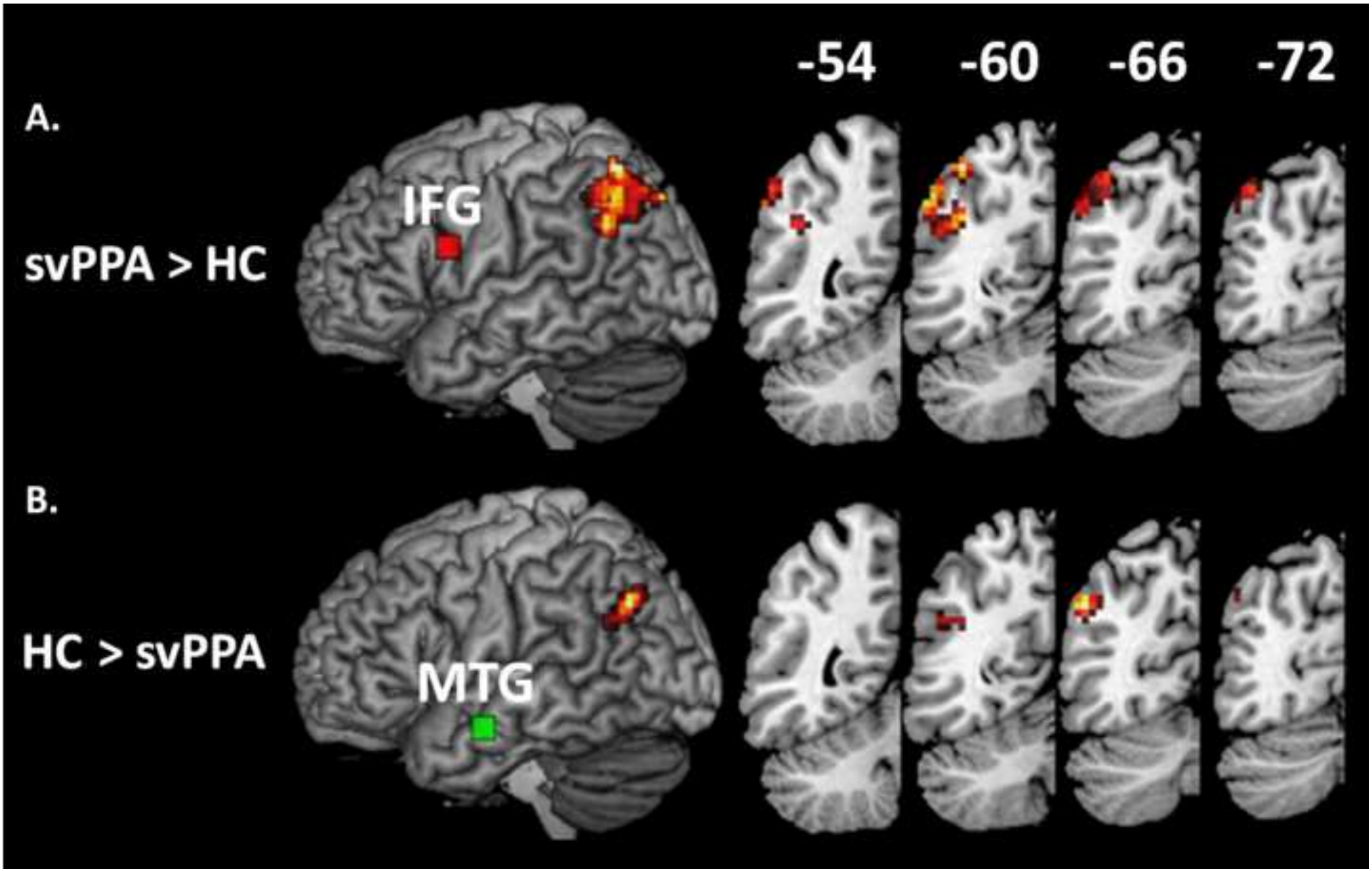

Figure 5

Click here to download high resolution image